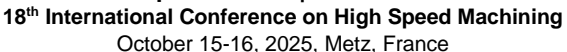


MM Science Journal | www.mmscience.eu

ISSN 1803-1269 (Print) | ISSN 1805-0476 (On-line)

Special Issue | HSM 2025



DOI: 10.17973/MMSJ.2025_11_2025141



HSM2025-44820

ENHANCED MATERIAL EFFICIENCY IN HYBRID MANUFACTURING THROUGH WIRE-BASED DED-LB AND NON-PARALLEL SLICING

F. Kalter^{1*}, J. Zarges^{1 * **}, S. Meiniger¹, K. Fey¹, M. Weigold¹

¹Technical University Darmstadt, Institute for Production Management, Technology and Machine Tools, Darmstadt, Germany

*Equal contribution

**Corresponding author; e-mail: J.Zarges@ptw.tu-darmstadt.de

Abstract

Hybrid manufacturing approaches, combining additive with subtractive manufacturing technologies, offer superior material efficiency compared to traditional subtractive manufacturing techniques. However, metal powder-based additive manufacturing methods reduce this advantage due to unavoidable powder loss. Additionally, most additive manufacturing processes necessitate the use of support structures to fabricate overhanging geometrical features, further compromising material efficiency.

This study presents a hybrid manufacturing strategy that employs a wire-based Directed Energy Deposition (DED-LB-w/M) process in combination with an 8-axis robotic system. The strategy aims to maximize material efficiency while maintaining geometric flexibility and accuracy. The system integrates a 6-axis robotic arm with a turn-tilt table, enabling the fabrication of overhangs without the need for additional support structures by applying a non-parallel slicing method. The developed strategy requires local control of the deposition rate to create a tilted layer surface while maintaining continuous deposition. First, we give an overview of robot-based hybrid manufacturing and its challenges followed by a description of the experimental setup. Based on this, the limitations of the robot system regarding dynamical behavior as well as positional accuracy and the resulting constraints to the permissible process parameters are investigated. Finally, the manufacturing strategy is validated by manufacturing demonstrator parts and analyzing the process stability as well as reproducibility.

Keywords:

Directed energy deposition (DED), Hybrid manufacturing, Process control, Robot

1 INTRODUCTION

Since its introduction in the 1980s through stereolithography [Yang 2017], additive manufacturing has experienced a continuous increase in popularity [Schneck 2021]. Regarding the number of publications, additive manufacturing is currently the fastest-growing field in production [Heiden 2025]. While it initially focused on plastic materials, the additive manufacturing of metals has become a key research factor in the generative production of parts with high mechanical strength and durability [Schneck 2021]. In the realm of metal-based additive manufacturing, Directed Energy Deposition (DED) is one of the most prominent manufacturing processes [Xu 2018]. DED tools allow an easy integration in manufacturing centers as well as in robot-based hybrid systems [Svetlizky 2021]. The latter is identified through the literature as one of the emerging trends of DED [Zhou 2024]. It addresses the process limitations regarding geometrical accuracy and surface roughness while simultaneously introducing a wide range of possibilities to improve material efficiency, geometric complexity, and the build volume of realizable

parts through a high degree of flexibility [Lalegani Dezaki 2022]. At the same time, hybrid manufacturing presents challenges due to increased system complexity.

The presented work explores the possibilities and challenges arising from robot-based hybrid manufacturing through the process of DED-LB-w/M. Stemming from the use of wire material, a material efficiency rate of nearly 100% can be achieved [Ahn 2021], [Bambach 2021], [Gibson 2021] while also resulting in a further increase in process complexity. A model-based approach is developed and utilized to predict the geometry of the build-up volume and to derive material-dependent process windows of stable generative deposition. Taking advantage of this approach, an adaptive open-loop control of the main process parameters is used to allow material deposition with an interlaminar change in layer height. Resulting from the non-parallel layers achieved through the adaptive process control in conjunction with the system's geometrical freedom, the manufacturing of complexly shaped parts with overhanging features without the need for support structures becomes feasible.

2 ROBOT-BASED HYBRID MANUFACTURING

2.1 Motivation: Material efficiency

One of additive manufacturing's main promises is a high degree of material efficiency without the need for specific tools [Gebhardt 2016]. This promise is contradicted by the need for support structures in overhanging regions, resulting in a decrease in material efficiency as well as in the need for post-processing steps for structure removal. Specifically in the case of metal-based additive manufacturing support structures are generally to be avoided, due to the high mechanical strength of the base material, resulting in limitations regarding the achievable geometrical complexity [Zhang 2022]. This dampens the widespread use of additive manufacturing technologies in industrial applications, as real-world components mostly show a high degree of geometrical complexity. To conquer this, the utilization of robot-based hybrid manufacturing systems is proposed. Generally, hybrid manufacturing refers to the combination of different manufacturing methodologies [Lalegani Dezaki 2022]. Especially the combination of additive and subtractive manufacturing can be identified as the focus of hybrid manufacturing literature [Lalegani Dezaki 2022], [Baier 2019], [Chen 2025]. With the potential of increased production flexibility and reduced material waste, additive manufacturing technologies are complemented by classical subtractive operations. In this way, the oftentimes lacking surface quality and geometrical accuracy of additively manufactured parts are elevated onto final component levels. The usage of industrial robots in hybrid manufacturing systems further facilitates production flexibility while simultaneously lowering investment cost [Baier 2019]. DED-LB-w with its high built rate and low integration cost into existing robot manufacturing systems is a promising AM technology in the context of hybrid manufacturing's core goal of operating cost optimization [Wang 2025]. In the presented work, the system's structure of a 6-axis industrial robot in combination with a 2-axis turntilt table is exploited to manufacture bent components through DED-LB-w/M without the need for support material, increasing the process's ability to manufacture complexly shaped parts.

2.2 Related Work

Utilizing systems like the previously described setup, different approaches towards support-free manufacturing of overhanging structures through DED have been proposed in the literature [Murtezaoglu 2018], [Assaad 2019], [Kaji 2023]. In contrast to the presented work, the usage of powder as the feeding material can be seen as the research standard. Kaji et al. for example utilize an 8-axis system to achieve bent geometries without the use of support material with a powder-based process [Kaji 2023]. The methodical basis distinguishes itself through advanced slicing methodologies that try to approximate a bent or sloped geometry through slices of variable layer height, resulting in a reduced discretization or cusp-height error compared to conventional slicing approaches as illustrated in the figure below.



Fig. 1: Discretization error of sloped geometry. Taken from [Shi 2020]

The avoidance of support material is achieved through the tilting of the substrate structure by a 2-axis turn-tilt table.

The main differences between the work presented and the findings by Kaji et al. result from the use of materials in

different base states and therefore in deviating process control conditions. Stemming from the use of powder material, a lower sensitivity of the process regarding process stability can be identified [Bambach 2021]. Excess material that is not melted by the energy source overshoots the workpiece, resulting in so-called overspray, that is not further affecting the generative manufacturing process [Ahn 2021]. Because of this, the powder-based process is less prone to destabilization through unwanted material buildup. Therefore, the work by Kaji et al. disregards the potential deviations between ideal and actual geometry.

While modelling strategies predict the dimensions and quality of individual beads and multi-track layers with given process parameters, the actual results may vary due to model uncertainties, unknown boundary conditions, or process anomalies. Furthermore, geometric models, which mostly cover single beads or simple layers, might not be valid for the deposition of arbitrary, sometimes complex geometries [Bernauer 2024]. The deviations of the layer height are especially critical since any error in the prediction adds up over the build process ultimately leading to wire dripping or stubbing as introduced in 4.1 [Heralić 2012; Abioye 2013].

This motivates the development of control strategies, which utilize sensor data as feedback. Process parameters and the trajectory of the laser processing head can be adapted to the as-build part in order to maintain a stable process and to increase the geometrical accuracy. The variety of controllers that can be found in literature can be distinguished between in-process control and inter-layer control. In-process measurements allow real-time control of one or more process parameters. When conducting measurements after the printing process of one layer has finished, inter-layer control can be used to calculate optimal parameters for the next layer [Bernauer 2024; Heralić 2012; Garmendia 2019]. The basic principle of the implemented compensation strategies will be discussed in 4.2 and 4.3.

2.3 Challenges

While then DED-LB-w/M has a high material efficiency rate of nearly 100% [Bambach 2021], [Ahn 2021], the resulting volume consistency leads to a small region of stability compared to powder based DED processes, which has a self-regulating effect [Bernauer 2024]. Therefore, not only the ideal but also the actual surface geometry has to be considered in the adaptive planning of process parameters to guarantee a stable multilayer deposition. In conjunction with this, a further challenge presents itself through the higher build volumes achieved through the wire-based manufacturing process. Resulting deviations between an ideal bent geometry and the discretization achieved through the developed slicing methodology have to be accounted for in the planning of consecutive layers. Finally, the kinematics of the 6-axis robot and the 2-axis turn-tilt table that are presented by the work of Kaji et al. have to be adapted and applied to the specific system used in this research. Because of the higher build volume, any deviation between the assumed and true orientation and position of the workpiece can lead to significant deviations in the final build component, making kinematic calibration crucial. Finally, all the described challenges have to be channeled into the development of a non-parallel slicing methodology that complies with the system and process limitations to allow the stable generative construction of complex 3D geometries.

3 NON-PARALLEL SLICING METHODOLOGY

Manufacturing parts using non-parallel slices enables the efficient and support-free build-up of complex geometries. In practice, this is achieved by utilizing the ability of the DED-LB-w/M process to change the local layer height by modifying the wire feed rate as well as the TCP speed. With that it is possible to deposit inclined weld tracks, that can be stacked to build curved geometries.

The greatest reachable angle of a single inclined track is limited by the reachable slope between the highest and lowest deposition height which in turn is limited by the process dynamics. Our developed method additionally utilizes a turn-tilt table that is tilted with the same slope angle as a deposited track. Thus, we ensure that the end effector's deposition direction always aligns with the direction of gravity. When this procedure is applied, a deviation between a given centerline of the profile and the actual centerline of the manufactured part occurs. This deviation is based on the discretization of the process, as each centerline of an individual slice is linear and not curved. Over time these discretization errors add up, leading to a substantial deviation from the target geometry. Therefore, the centerline of the discretized layer is shifted to the centerline of the target geometry to minimize the discretization error. A visualization of the error summation over multiple layers is sketched out in Fig. 3. Together with potential geometric deviations of the individual slices based on process variations (see 4.2), the decision was made to use an online slicing approach, which reslices the target geometry after each 3D-Scan.

The non-parallel slicing methodology requires the process and reference plane (see Fig. 4) to be tilted with respect to each other. Due to the volume consistency of the wire-based DED process, the deposition rate needs to be adapted along the deposition trajectory to produce a layer of varying thickness. The deposition rate in turn depends on the process parameters v_{tcp} and v_{wire} . In order to find optimal process parameters the trajectory is discretized into individual trajectory points. The target, local layer height at each trajectory point i can be calculated from the normal

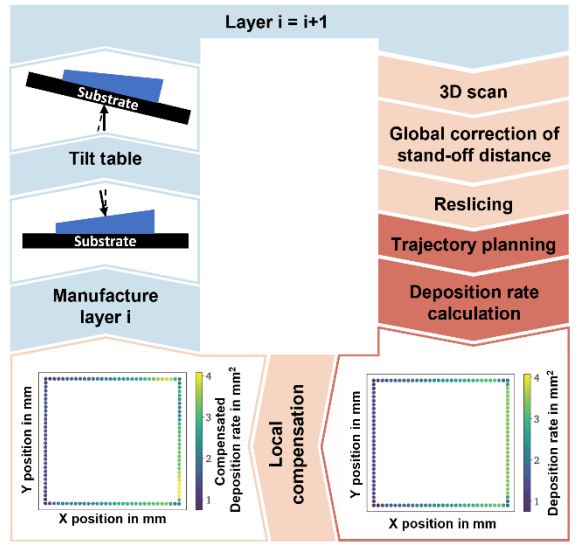


Fig. 2: Diagram of the manufacturing process of tilted structures. Red: Pre-processing, light red: Adaptive compensation, blue: Processing.

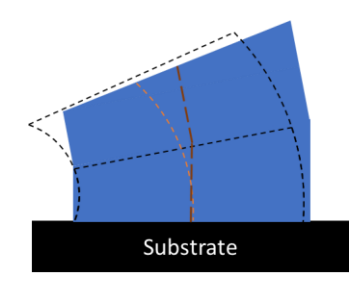


Fig. 3: Error buildup. The orange dotted line represents the centerline of the target geometry, while the red dashed line is the centerline of the manufactured layers.

distance of the processing plane to the reference plane. The process parameters $v_{tcp,i}$ and $v_{wire,i}$ can be calculated numerically by minimizing the difference of the target height $h_{\rm i}$ and the modeled layer height $h_{\rm b}(v_{tcp},v_{wire})$ (see 4.1) and the weld bead width w_i respectively (see 4.1) using SciPy-optimise function fsolve. The start point of the deposition is chosen in the area of maximum deposition rate, which corresponds to the minimal permissible trajectory speed $v_{tcp, \min}$ and maximum permissible wire speed $v_{wire, \mathrm{max}}.$ The value pair is used as an initial value for the optimization. For all following trajectory points i the value pair $[v_{tcp,i-1}, v_{wire,i-1}]$ is used as an initial value. To ensure a stable deposition within the qualified process window (see 6.1), a linear constraint is added to the process parameters, which can be described by a straight line connecting the points $[v_{tcp,min}, v_{wire,max}]$ $\left[v_{tcp,max},v_{wire,min}\right]$ in the design space.

4 DEVELOPMENT OF LOCAL LAYER HEIGHT CONTROL

4.1 Model for Layer height

The DED-LB-w/M process is especially sensitive to process errors caused by an incorrect stand-off distance between the nozzle and the workpiece [Garmendia 2019]. If the stand-off distance is too big the wire material melts above the workpiece surface leading to the characteristic error called dripping. If the stand-off distance is chosen too small, the insufficiently melted wire can stick to the surface, often referred to as stubbing. Therefore, it is critical to obtain a model that allows for an accurate prediction of the deposited weld bead geometry and the layer height based on the process parameters and the thermal boundary conditions. Previous work at the institute showed that Buckingham-Pi models serve as an efficient yet accurate method to predict weld bead height. Furthermore, they can be easily extended with additional parameters and allow a direct integration of the physical properties of the used material. To obtain the Buckingham-Pi parameters the process parameters laser power P_L , the trajectory speed v_{tcp} , the feed rate of the wire v_{wire} and laser beam diameter d_{laser} such as the material-specific parameters heat capacity c_n , heat conductivity λ and the temperature difference between the substrate and the melting point of the deposited material ΔT are chosen as free parameters, while the weld bead height h_b and the weld bead width w_b represent the dependent parameters. The parameters are combined to obtain the dimensionless Buckingham Pi

$$\Pi_{1,h} = \frac{h_b \, v_{tcp} \, \rho \, c_p}{\lambda} \tag{1}$$

$$\Pi_{1,w} = \frac{w_b \, v_{tcp} \, \rho \, c_p}{\lambda} \tag{2}$$

$$\Pi_2 = \frac{d_{laser} \, v_{tcp} \, \rho \, c_p}{\lambda} \tag{3}$$

$$\Pi_3 = \frac{P_{laser} \, v_{tcp} \, \rho \, c_p}{\lambda^2 \Lambda T} \tag{4}$$

$$\Pi_4 = \frac{v_{wire}}{v_*} \tag{5}$$

Best results were achieved for a multiplicative approach. The model has been fitted across three different materials resulting in an adjusted R^2 of 0.929 and an RMSE of 0.097 mm. However, the model proved to be less accurate in predicting the weld bead width with an adjusted R^2 of 0.722 and RMSE of 0.238 mm.

4.2 Interlaminar correction of the stand-off distance

The error of the modelled layer height can be compensated by controlling the process parameters to track the reference height or by adjusting the vertical offset of the next process plane to the actual mean layer height of the current layer. The latter approach minimizes the required control action and thus the deviations from the qualified nominal process parameters [Heralić 2012]. Also, it does not depend on the model error, thereby ensuring minimal defocus of the laser for all layers. Consequently, this approach is implemented to cope with unintended over- or under-build in all layers. The basic principle of the global trajectory offset adaption is illustrated in Fig. 4. After the deposition of each layer, its surface topography is obtained by means of a 3D scanner. The mean error of the layer surface to its reference plane. denoted as Δh_{alohal} , is determined with a ray-casting method. The mean of all acquired ray-casting distances to the layers process plane reflects the mean layer height. Before the next layer is manufactured its process plane is offset by the mean height error in its normal direction, minimising the local standoff error along the deposition trajectory.

4.3 Local layer height compensation

While the presented method allows for a model-based calculation of nominal process parameters, the actual deposition rates need to be adapted to compensate local variations $\Delta h_{local,i}$ from the mean layer height (see Fig. 4), measured by the 3D-scanner as described in the previous section. The local deviations occur due to the limitations of the system dynamics (see 6.2), thermal effects or process anomalies. The compensated process parameters can be obtained by adding the local errors $\Delta h_{local,i}$ to the target height h_i . An example of the compensated deposition rates can be seen in Fig. 2. The superposition of the local errors lead to a reduction of the deposition rate in the area of corner points and the start point of the previous layer where an overbuild can be observed due to the inertia of the robotic system. Respectively an under build will lead to an increase of the deposition rate in the following layer. In order to allow control action at the point of min/max deposition rate, the permissible interval is reduced with respect to the qualified process window described in 6.1. This enables the system to react to any variations of the surface topography of the build part, stabilizing the deposition process and preventing an unwanted local accumulations of material.

5 EXPERIMENTAL SETUP

The experimental setup used in this study consists of mainly two parts, a *robot cell* as well as a *3D-Scanner* setup, both are visualized and described in the following subsections. The experiments conducted in this study consist of the processing of a layer, followed by a short wait time and a subsequent 3D scan. This way we can make sure that each layer cools down to approximately room temperature, so that the scan results are not influenced by heat accumulation.

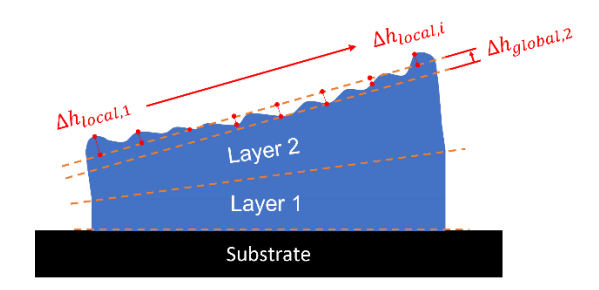


Fig. 4: Global and local error of a discrete trajectory pints i. Adapted from [Garmendia 2019] and [Bernauer 2024].

5.1 Robot system

The robot cell consists of an ABB IRB 6660-205 industrial robot as well as a turn-tilt table for 8-axis machining. The process optic is a Coaxworks wireM with a 3-Beam system utilizing a 4kW diode laser source. The material in use for all experiments is In718 wire with a 1.2 mm diameter. A schematic drawing of the cell can be seen in *Fig. 5*.

5.2 3D-scanner

For 3D-scanning a KScan Magic with an accuracy of 0.01 mm is used. The scanner is placed on a tripod in front of the turn-tilt table that continuously moves the part following a standardized routine. This is done to prevent influences of movement or scan strategy on the result and keep the comparability as high as possible between experiments. To conduct the scan the placement of markers around the substrate plate is necessary.

6 SYSTEM CONSTRAINTS

As stated in section 3, the achievable slope in a single layer and thus the producible geometry is restricted by multiple system characteristics like the dynamics of the robot or the stable process parameter boundaries. In the following section, we will investigate the different constraints and assess geometric limitations for the experiments in section 7.

6.1 Process window

The theoretically achievable geometries of the deposited weld beads are constricted by the process window in which stable deposition is possible. In general, the permissible process window depends on the characteristics of the used material, the thermal boundary conditions and the configuration and dynamics of the used manufacturing system. In previous work at the Institute process windows have been qualified for various materials including Inconel 718, which is used for the validation experiments in chapter 8 since it allows for stable, defect free deposition in a large domain of the investigated process Parameters P_{laser} , d_{laser} , v_{tcp} and v_{wire} .

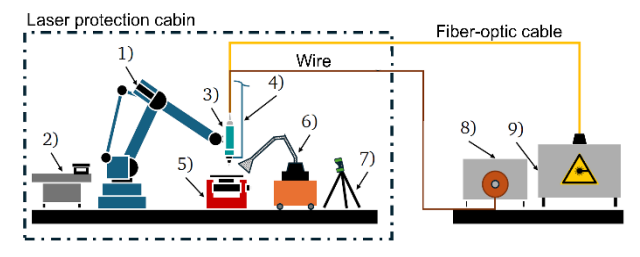


Fig. 5: (1) ABB Robot, (2) Rack for motor spindle, (3) COAXwire processing head, (4) Shielding gas, (5) Turn tilt table, (6) Fume extraction, (7) KScan Magic 3D-scanner, (8) DINSE Wire feeder, (9) Laserline Diode Laser.

The material qualification process consisted of a series of single bead experiments, varying the combined parameters of line energy E_L and energy per deposited volume E_V . Parameter sets that resulted in instabilities or pores in the weld bead were rejected. Hence, the resulting process window can be described by the minimum and maximum of the energy terms E_L and E_V . The ratio of E_L and E_V is referred to as the deposition rate V [Abioye 2013]. By using the model described in chapter 5.1, a minimal layer height $h_{b,min}$ of 0.343 mm and a maximum layer height of $h_{b,max}$ of 1.417 mm can be calculated. The theoretical slope angle $\Delta \phi$ that can be achieved by varying the deposition rate in the permissible range over the distance s can therefore be derived with

$$\Delta \varphi = \arctan(\frac{h_{b,max} - h_{b,min}}{s})$$
 (6)

6.2 System dynamics

In our presented method, the generation of a slope is realized by changing the deposition rate along a given trajectory. Due to the dynamics of the robotic system, it is not possible to manufacture arbitrary slopes, thus the real deposition behavior needs to be assessed. Based on the process window the maximum and minimum deposition rates are set and the resulting TCP velocity and wire feed rate are derived. The first experiments solely focused on the robot dynamics and it was found that a distance of 8 mm is sufficient to ensure, that the robot reaches the targeted velocities in any given direction. Note that this holds only true for the given min/max TP velocities as well as robot poses close to the used workspace (i.e. above the turn tilt table). Afterward, multiple single-line weld tracks were manufactured to test, the influences of the wire feed inertia on the system. The track geometry starts at the maximum deposition rate and is kept constant for 11 mm, then the deposition rate is decreased over 8 mm to the minimum value and is kept constant for 22 mm before it increases again over 8 mm. Fig. 7 depicts the height profile of ten weld tracks. A comparison between the target and actual geometry averaged over 20 weld tracks can be seen in Fig. 8. We can clearly see an accumulation of material at the start of each weld track, due to the robots inertia. Our system is unable to start processing in a fly-by fashion thus, the initial TCP velocity is 0 resulting in very high deposition rates. Furthermore, we can see that the actual geometry is slightly offset to the left with material build-up right before the deposition rate increases again. The cause for this is likely the approximation zones in the robot path trajectory for smooth movements. Overall, we have found that the wire feed inertia does not impact the process and that a distance of 8 mm is still sufficient to ensure the robot can follow a target geometry. Given that and the maximum achievable difference in deposition rate, the achievable slope per layer is approx. 7.6° as given by equation 6. Due to the experienced material accumulation though, this value is not stable as it prevents possible error corrections in later layers as it operates at the edge of the stable process window. Hence the maximum achievable deposition rate difference is reduced resulting in a slope of approximately 3.8° per layer, giving enough room for corrections in the following layers.



Fig. 6: Hollow rectangular profile with a curvature of 20°.

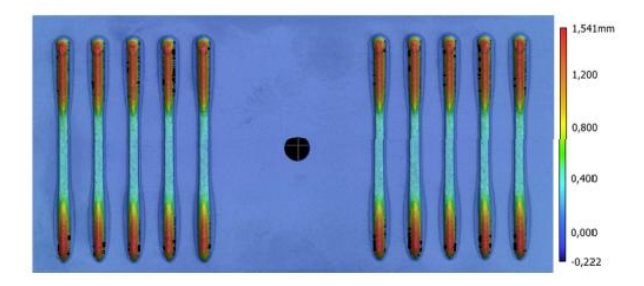


Fig. 7: Height profiles of 10 weld tracks used to determine the system dynamics for a maximal variation of the deposition rate.

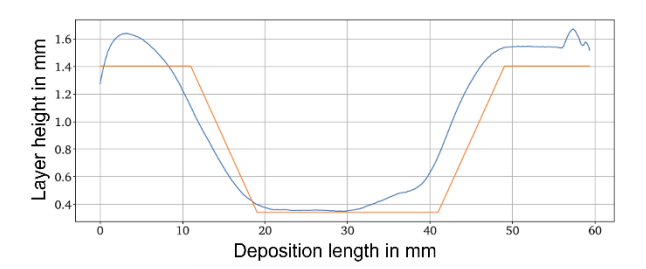


Fig. 8: Actual height profile of the welding tracks averaged over 20 single lines (blue). Nominal height profile (orange).

6.3 Positional accuracy

While the robotic system has many benefits like large and flexible workspaces, it comes at the cost of a reduced positional accuracy compared to traditional machine tools. The positional accuracy of our method is mainly influenced by two factors, the accuracy of the kinematic chain itself i.e. the robot and the turn tilt-table joint accuracy on one hand and on the other the localization of the turn-tilt table axis in space to derive the transformation matrices from for position calculation. The former is given by the manufacturer, while the latter needs to be evaluated. To do this the axis positions were measured with a Wiest AG LaserLAB measuring system before a comparison between actual tilt-turn position and theoretical tilt-turn position was performed. Results show a deviation of about 0.115 mm for a point approx. 20 mm above the table surface when it is tilted 75° around both its rotational axis. This deviation is not critical for the current use case but can prove challenging when manufacturing larger parts, as the deviation will grow with the distance towards the turn-tilt table.

7 VALIDATION EXPERIMENTS

To assess the performance of our developed method multiple validation parts are manufactured. We decided on a hollow rectangular profile with an edge length of 30mm and a slope of 1.25° per layer with a target curvature of 20°. To be able to assess process stability 6 validation parts are manufactured. Beyond the geometrical accuracy we also evaluate the reproducibility of a part based on its actual trajectories and process data obtained during manufacturing.

7.1 Geometrical accuracy

The first finding of the validation experiments is that we need more layers than theoretically need to manufacture a part, due to the re-slicing utilized in our method as well as the deposition rate compensation. With the geometry of our part 16 layers should mathematically be sufficient, yet all parts needed 19 layers to be manufactured. To assess geometrical accuracy, we measure the local relative

geometric error ΔH_{local} . This metric provides a mean global error but also an estimate of process stability as well as an indication of critical sections of the validation parts. To calculate it we first discretize the trajectory with a resolution of 0.5 mm. Next the actual geometry is measured using the 3D scanner and the absolute local error Δh_{local} is calculated for each trajectory point T_i by averaging the error of an rectangular neighborhood around T_i with edge length 0.5mm. Lastly the maximum tolerated error $h_{\rm lim}$ for each T_i needs to be calculated. It is given by the difference between target deposition rate and min/max deposition rate and describes the error that leads to leaving the stable process window. Whether the upper or lower tolerated error is chosen depends on the sign of Δh_{local}

$$H_{lokal,i} = \frac{h_{lokal,i}}{h_{lim,i}} \tag{7}$$

$$h_{lim,i} = h_{max} - h_{soll,i} \text{ or } h_{soll,i} - h_{min}$$
 (8)

This means that -1< ΔH_{local} < 1 is a stable region, where occurring deviations can be compensated in the following layer.

As can be seen in Fig. 9, most relative errors are close to zero, and the vast majority is in the range of -1 to 1, indicating a stable deposition process. However large deviations, that cross the threshold for stability, can be identified at the corners of the geometry. Most notably at corners, in the region of minimal deposition rate. While this is not surprising, it shows that the current corner compensation method used in our approach is not necessarily suitable for manufacturing more complex geometries. However, the stable manufacturing of the validation part was still possible, as error propagation was prevented by the local compensation. Lastly, compare the manufactured part with the target geometry. Fig. 10 shows, that the areas most impacted by errors are along the edges of the last layer, as well as left and right of the profile corners, while the vast majority of the part shows no, to very little deviation.

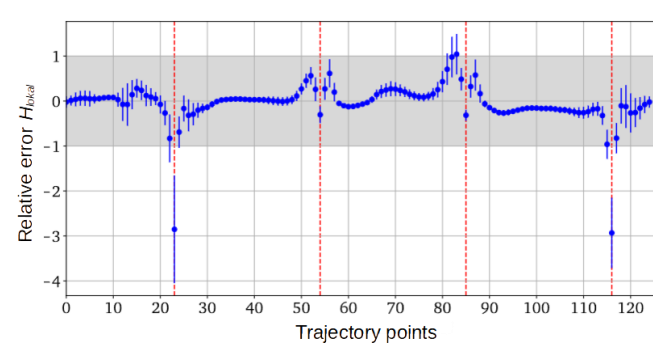


Fig. 9: Relative error, along the manufactured contour. The dotted red lines indicate the corners.

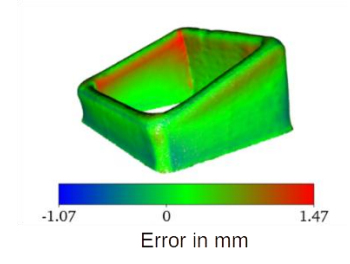


Fig. 10: Geometric error of as-build part to target geometry.

7.2 Reproducibility

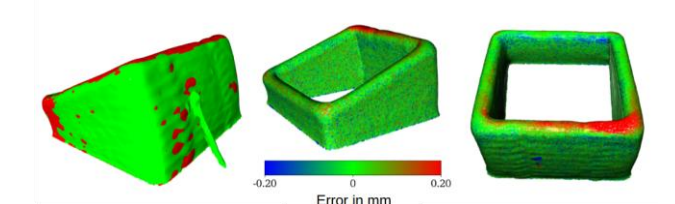


Fig. 11: Geometric error between cloned instances. The process error seen on the left had no noticeable impact on the accuracy.

One notable downside of our proposed method is that the 3D scan after each manufactured layer takes significant time, approximately 2 minutes for the validation part. This reduction in productivity might not be suitable for real world applications, so the question arises what we can do to circumvent that problem. If the process is stable enough and does not show a high amount of statistical anomalies, one potential solution is to clone the manufacturing data from a successfully manufactured part, to fabricate an additional instance. This includes the trajectory data as well as all process data for each trajectory point like wire feed rate, laser power etc. The result of this approach is depicted below. We can see that the error between different instances manifests mainly around the start stop point for each layer, and again around the corners of the profile. Most notably a process error at the laser start occurred in layer 12, yet the part could still be manufactured and the self-healing effects of the process prevented the propagation of errors in later layers. Overall, we can clearly assess that our proposed methodology not only enables us to manufacture curved geometries without support structures but is also robust enough to allow for straightforward re-usability of parameters for a qualified

8 SUMMARY AND OUTLOOK

In this study we introduced a novel method to realize the manufacturing of complex overhang structures with wire based DED-LB process, without the need for support structures. First the developed method was explained and set into context of the wider research field of non-parallel before introducing additional compensation strategies to make the method more robust. Next the system constraints have been discussed as they set the limit of which geometries can be potentially realized. Based on these constraints a validation geometry was chosen and manufactured multiple times to assess performance and stability of the proposed non-parallel slicing method. It was shown that the process is stable with the exception of singular small areas at the corners of the geometry while producing geometric errors smaller than 0.15 mm. Additionally the process proves robust enough to allow for a re-usability of the process strategies for qualified parts. However, some questions and tasks remain open. First and foremost, it was made clear that corners are the most critical areas of a part, so a more sophisticated compensation approach for corners might be needed when more complex profiles or contours are to be manufactured. Next the problem of decreasing positional accuracy with increasing distance from the substrate surface needs to be considered as an obstacle to manufacture large volume parts where a robotic system could truly show its advantages in workspace size and flexibility.

9 REFERENCES

[Abioye 2013] Abioye, T.E. et al. A parametric study of Inconel 625 wire laser deposition. Journal of Materials Processing Technology, 2013, Vol. 213, No. 12, pp. 2145–2151. ISSN 0924-0136.

[Ahn 2021] Ahn, D.-G. Directed Energy Deposition (DED) Process: State of the Art. International Journal of Precision Engineering and Manufacturing-Green Technology, 2021, Vol. 8, No. 2, pp. 703–742. ISSN 2198-0810.

[Assaad 2019]. Design and Pathway Programming of Freeform Thin-walled Geometries Produced by Laser Metal Deposition. In: D. Di MECCANICA; 531; dell'informazione, AREA MIN. 09 - Ingegneria industriale e; N. assegn, eds. Proceedings of LiM 2019—Lasers in Manufacturing. 2019, pp. 1–10.

[Baier 2019]. Robot-Based Hybrid Production Concept. In: J.P. Wulfsberg; W. Hintze; B.-A. Behrens, eds. Production at the leading edge of technology: Proceedings of the 9th Congress of the German Academic Association for Production Technology (WGP), September 30th - October 2nd, Hamburg 2019. Berlin, Heidelberg: Springer. 2019, pp. 451–460. ISBN 978-3-662-60417-5.

[Bambach 2021] Bambach, M. et al. Directed energy deposition of Inconel 718 powder, cold and hot wire using a six-beam direct diode laser set-up. Additive Manufacturing, 2021, Vol. 47, p. 102269. ISSN 2214-8604.

[Bernauer 2024] Bernauer, C. et al. Segmentation-based closed-loop layer height control for enhancing stability and dimensional accuracy in wire-based laser metal deposition. Robotics and Computer-Integrated Manufacturing, 2024, Vol. 86. ISSN 07365845.

[Chen 2025] Chen, Y. et al. Five-axis hybrid manufacturing with DED and milling for complex multi-branched metallic parts. International Journal of Computer Integrated Manufacturing, 2025, pp. 1–30. ISSN 0951-192X.

[Garmendia 2019] Garmendia, I. et al. Development of an Intra-Layer Adaptive Toolpath Generation Control Procedure in the Laser Metal Wire Deposition Process. Materials (Basel, Switzerland), 2019, Vol. 12, No. 3. ISSN 1996-1944.

[Gebhardt 2016]. 3D-Drucken: Grundlagen und Anwendungen des Additive Manufacturing (AM). München: Hanser, 2016. ISBN 9783446446724.

[Gibson 2021]. Additive manufacturing technologies. Cham: Springer, 2021. ISBN 9783030561277.

[Heiden 2025]. Chapter 13 - Additive Manufacturing (AM) and AI. In: D.A. Lamprou, ed. Fundamentals and Future Trends of 3D Printing in Drug Delivery. Chantilly: Elsevier Science & Technology. 2025, pp. 283–304. ISBN 978-0-443-23645-7.

[Heralić 2012] Heralić, A. et al. Height control of laser metalwire deposition based on iterative learning control and 3D scanning. Optics and Lasers in Engineering, 2012, Vol. 50, No. 9, pp. 1230–1241. ISSN 0143-8166.

[Kaji 2023] Kaji, F. et al. Robotic laser directed energy deposition-based additive manufacturing of tubular components with variable overhang angles: Adaptive trajectory planning and characterization. Additive Manufacturing, 2023, Vol. 61, p. 103366. ISSN 2214-8604.

[Lalegani Dezaki 2022] Lalegani Dezaki, M. et al. A review on additive/subtractive hybrid manufacturing of directed energy deposition (DED) process. Advanced Powder Materials, 2022, Vol. 1, No. 4, p. 100054. ISSN 2772-834X.

[Murtezaoglu 2018] Murtezaoglu, Y. et al. Geometry-Based Process Planning for Multi-Axis Support-Free Additive Manufacturing. Procedia CIRP, 2018, Vol. 78, pp. 73–78. ISSN 2212-8271.

[Schneck 2021]. Technology strategy for metal-based additive manufacturing. Dissertation. Technische Universität München, 2021.

[Shi 2020] Shi, T. et al. Precise control of variable-height laser metal deposition using a height memory strategy. Journal of Manufacturing Processes, 2020, Vol. 57, pp. 222–232. ISSN 15266125.

[Svetlizky 2021] Svetlizky, D. et al. Directed energy deposition (DED) additive manufacturing: Physical characteristics, defects, challenges and applications. Materials Today, 2021, Vol. 49, pp. 271–295. ISSN 1369-7021.

[Wang 2025] Wang, L. and Wang, F. Optimization of operating costs for hybrid manufacturing production mode based on wireless sensor networks and robots. The International Journal of Advanced Manufacturing Technology, 2025, pp. 1–11. ISSN 1433-3015.

[Xu 2018] Xu, J. et al. A review of slicing methods for directed energy deposition based additive manufacturing. Rapid Prototyping Journal, 2018, Vol. 24, No. 6, pp. 1012–1025. ISSN 1355-2546.

[Yang 2017]. Additive manufacturing of metals: the technology, materials, design and production. Cham: Springer, 2017. ISBN 9783319551289.

[Zhang 2022] Zhang, J. et al. A review on design and removal of support structures in metal additive manufacturing. Materials Today: Proceedings, 2022, Vol. 70, pp. 407–411. ISSN 2214-7853.

[Zhou 2024] Zhou, L. et al. Additive Manufacturing: A Comprehensive Review. Sensors, 2024, Vol. 24, No. 9, p. 2668. ISSN 1424-8220.